JOURNAL OF MATERIALS SCIENCE 20 (1985) 1787–1793

Field-induced silver injection into lithium disilicate glass

A. DOI
Department of Inorganic Materials, Nagoya Institute of Technology, Nagoya 466, Japan
T. MIWA, A. MIZUIKE
Faculty of Engineering, Nagoya University, Nagoya 464, Japan

The objective of this work was to study field-induced silver injection into $Li_2O \cdot 2SiO_2$ glass by the techniques of secondary ion mass spectrometry and thermally stimulated polarization/depolarization current (TSPC/TSDC), with an emphasis on the comparison experiments between gold and silver electrodes. For both anode materials, accumulation of lithium was found near the cathode. The blocking nature of the gold anode was demonstrated by the closeness of the observed and estimated width of the alkali-depleted region near the anode. For silver-anode samples, field-induced silver injection as well as lithium conduction occured and increased the TSPC slope from that of the gold-anode samples.

1. Introduction

Heavy metals, such as nickel, molybdenum and niobium, can be injected into glass if they are in the monovalent state [1]. Silver is the most mobile of those metals when incorporated into glass because of its small ionization potential and ionic radius. Yet silver is not so unique in diffusion characteristics, since the diffusion coefficient of silver ions is comparable with that of sodium ions in pyrex [2, 3] or sodium borate [4] glasses, or even less than that of lithium ions in lithium disilicate glass [5]. Although the diffusion kinetics of silver into glass have been studied extensively from, for example, ion exchange reactions at the glass-electrolyte interface, studies on field-induced silver injection [5, 6] or silver implantation [7] into glass are rather limited.

Silver enters the glass from the surface, irrespective of any motive force for silver transport. Hence secondary ion mass spectrometry (SIMS) is particularly suited for studying the phenomena occurring at glass surfaces [8]. The present work was undertaken concerning d.c. field-induced silver injection into glass by the thermally stimulated polarization/depolarization current (TSPC/TSDC) techniques [9] in conjunction with SIMS. This is the extension of previous TSPC/TSDC studies [10, 11] on alkali silicate glasses and their polarization behaviour. There it was revealed the existence of three different polarizations named P1, P2, and P3 in the order of increasing peak temperatures within the temperature range of 80 to 700 K. The P1 peak was assigned as due to conduction polarization [12] of alkali ions, the P2 peak to conduction polarization of the nonbridging oxygen ions within the alkali-depleted region (ADR) near the anode, and the P3 peak to space charge polarization caused by space charge built near the electrodes during polarization which eventually leads to restriction on alkali conduction, hence generating the current peak. In those works circular gold electrodes were usually used but, when silver instead of gold was used as the anode, P2 was drastically reduced. This was explained [11] by charge compensation of the nonbridging oxygen ions within ADR by injected silver. The purpose of the present work was to obtain further information concerning field-induced silver injection into glass, with an emphasis on the comparison experiments between gold and silver electrodes.

2. Experimental procedures

Annealed samples of lithium disilicate glass, $Li_2O \cdot 2SiO_2$, were investigated. For some samples

0022–2461/85 $03.00 + .12

the glass ingot was crushed and remelted a second time for improving homogeneity. Those homogenized glass samples showed no striae. Glass discs 1 to 2 mm thick with an area of 0.50 cm^2 were provided with electrodes of evaporated gold, silver, or silver paste over the entire optically polished surfaces. Platinum foils with lead wires were placed over the electrodes. A disc was then clamped between two ceramic heaters and placed in a measuring cell which was evacuated by an oil-diffusion pump. In a TSPC measurement, the sample was cooled to 170 K where 200 V cm^{-1} was applied. The heating rate was not ideally linear but averaged 0.1 deg sec^{-1}. After heating to 500 K or some lower temperatures when specified, the sample was quenched to 170 K and reheated a second time without field (TSDC). An induced current during TSPC/TSDC run was detected with a Takeda Riken TR-8651 electrometer.

Polarized samples after TSPC runs were used for SIMS measurements. A Hitachi IMA-2 instrument with residual vacuum of about 1×10^{-5} Pa or less was used. The samples were bombarded with 8 to 15 keV Ar^+ ions, 0.25 to 0.87 mm in spot diameter and a beam current of 0.050 to 0.150 μA, and the positive secondary ions were analysed. Geometries of the sputter craters were measured with a Talysurf 10 surface texture measuring instrument. Ion bombardment is likely to induce surface charging that may cause the original profiles, especially of alkali ions, to change [8, 13, 14]. In our initial experiments, the charging effect caused endless decrease of the intensity of lithium with depth for even an unpolarized sample, even in the presence of electron spraying. This charging effect was greatly reduced by leaking the surface charge to the sample holder through painted silver paste and evaporated gold. Since lithium and silver are the dominant mobile species embedded in an immobile silicon network, the ordinate of our depth profiles is represented by the ratio of the SIMS intensity of those ions to that of silicon ions. However, the ratio depends on the selected energy window of the instrument which extracts the secondary ions of particular energy from those of broad energy distribution, because the distribution is affected by the parameter ρ [15] which represents the electron-spray current density divided by the primary ion current density. So the energy window was selected at the most probable energy of $^{28}Si^+$ ions, with ρ fixed at unity.

3. Results

Samples are labelled as e.g. Ag–Au (3) for sample no. 3 with a silver anode and gold cathode. Fig. 1 shows typical TSPC curves for Au–Au and Ag–Au samples, as well as linear portions of the TSPC curves for two Au–Au samples within which linear portions for other gold-anode samples lie. Reported conductivities for $30Li_2O \cdot 70SiO_2$ glass with a slope of 61.1 kJ mol^{-1} [16] (curve A) or 62.4 kJ mol^{-1} [17] (curve B) are also shown. A dominant TSPC peak at around 410 ± 20 K for a gold-anode sample is designated as P3. The TSPC data are summarized in Table I for three electrode pairs. Similar data on sodium disilicate glass are given in Table II for comparison.

The general results observed are as follows.

1. The magnitude and the slope of linear portions of the TSPC curves for gold-anode samples, with or without striae, were scattered from sample to sample and no systematic change was observed with sample thickness.

2. The TSPC slopes for silver-anode samples were always higher than those for gold-anode ones which were close to the reported activation energy for lithium conduction.

3. For gold-anode samples the TSPC current showed slow decrease after respective P3 peak maximum, while for silver-anode samples the

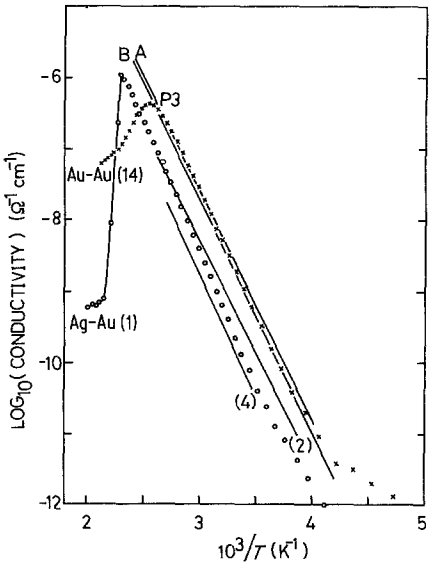

Figure 1 Typical TSPC curves for Au–Au (14) and Ag–Au (1), and linear portions of the TSPC curves for Au–Au (2) and (4) within which linear portions of the TSPC curves for other Au–Au samples lie. Curves A and B are reported d.c. conductivities for $30Li_2O \cdot 70SiO_2$ glass [16, 17].

TABLE I Summary of TSPC data for $Li_2O \cdot 2SiO_2$ glass with various electrode pairs. Q_p is the charge flowing during TSPC run up to peak maximum

Sample		Thickness (mm)	TSPC slope (kJ mol^{-1})	P3 peak temp. (K)	Q_p (C cm^{-2})	Comments
Au–Au	(1)	0.81	67.8	406	9.79×10^{-3}	
	(2)	0.87	62.0	425	2.29×10^{-2}	
	(3)	1.02	63.2	416	1.08×10^{-2}	
	(4)	1.09	64.5	–	–	TSPC up to 373 K
	(5)*	1.13	67.8	400	1.38×10^{-2}	
	(6)*	1.17	†	413	2.90×10^{-2}	RT to 500 K; $E_p = 256$ V cm^{-1}
	(7)*	1.18	63.6	403	1.08×10^{-2}	
	(8)*	1.18	63.2	418	1.02×10^{-2}	
	(9)	1.43	65.3	422	1.52×10^{-2}	
	(10)*	1.70	†	424	2.50×10^{-2}	RT to 500 K
	(11)	1.72	69.1	421	1.92×10^{-2}	
	(12)*	1.88	†	391	2.13×10^{-2}	RT to 500 K
	(13)*	1.98	†	405	2.88×10^{-2}	RT to 500 K
	(14)	2.60	64.0	396	2.50×10^{-2}	
Ag–Au	(1)	0.95	68.7	436	5.32×10^{-2}	
	(2)	1.02	73.3	460	8.66×10^{-2}	Ag-paste as anode
	(3)	1.09	68.2	–	–	TSPC up to 373 K
	(4)	1.09	74.1	479	4.98×10^{-1}	Ag-paste as anode
	(5)*	1.13	67.8	439	6.20×10^{-2}	
	(6)*	1.18	70.3	436	5.04×10^{-2}	
	(7)	1.30	71.6	433	1.36×10^{-1}	Ag deposited more than double the usual quantity
Ag–Ag	(1)	1.70	79.5	421	2.39×10^{-2}	
	(2)	1.75	87.1	438	8.41×10^{-2}	
	(3)	1.80	76.6	–	–	TSPC up to 394 K
	(4)	1.85	72.8	402	2.56×10^{-2}	

*Homogenized glass samples.
†Owing to narrow temperature range, reliable values of the slope were not obtained.

current suffered drastic degradation as shown in Fig. 1. When the amount of degradation was extremely large, the current became noisy after the degradation.

4. Q_p, the charge flowed in the external circuit during a TSPC run up to peak maximum, was larger for silver-anode samples than for gold-anode ones, and was larger when deposited silver was thicker.

Fig. 2 shows the TSDC curves for Au–Au sample after TSPC runs up to two different temperatures. The TSDC peak near 273 K is designated as P2. The charge flowed during the TSPC run up to 373 K (Case b-b′) was only 7.3% of the charge for the case a-a′, where the TSPC run up to 500 K was made. It is interesting to note that the TSDC current in the low-temperature range, other than P2, was always higher for the case b-b′ than for the case a-a′.

Figs. 3 and 4 show typical depth profiles of lithium and silicon near the electrodes after polarizing the Au-Au sample up to 500 K, with an overall charge of 4.98×10^{-2} C cm^{-2} which flowed during the TSPC run. Since the relative

TABLE II Summary of TSPC data for $Na_2O \cdot 2SiO_2$ glass with various electrode pairs

Sample		Thickness (mm)	TSPC slope (kJ mol^{-1})	P3 peak temp. (K)	Q_p (C cm^{-2})
Au–Au	(1)	1.53	69.1	375	7.26×10^{-3}
	(2)	1.75	70.3	397	1.85×10^{-2}
	(3)	1.80	61.1	362	2.58×10^{-3}
Ag–Au	(1)	2.33	88.7	417	2.28×10^{-2}
Ag–Ag	(1)	2.26	82.9	414	3.85×10^{-2}

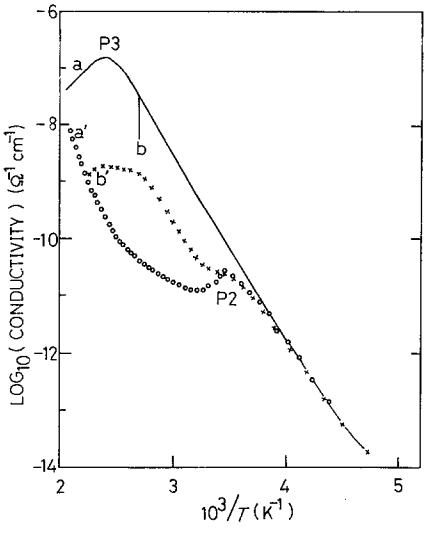

Figure 2 TSPC/TSDC curves for Au–Au (8) where the sample was polarized up to 500 K (a-a') or to 373 K (b-b'). Primes indicate TSDC curves.

sensitivity factor of gold is far below that of silver [18], we could not detect a SIMS signal of Au^+ even from the gold electrode. Fig. 5 shows a comparison of the depth profiles of lithium at the cathode and the anode for another polarized Au–Au sample. As the SIMS intensity of lithium for the previously unpolarized sample was almost depth-independent (Fig. 6), the profiles illustrate the presence of ADR and of alkali-accumulated region (AAR) near the cathode which developed by polarization. At the anode, the intensity of lithium increases gradually with depth, eventually comes to saturation which possibly represents the bulk. At the cathode, the intensity of lithium passes through minimum and reaches saturation.

When we changed positions of ion bombardment on the surface, the observed intensity of lithium at saturation decreased gradually (Figs. 3 and 6). Fig. 3 also illustrates shift of ADR to deeper depth with changing positions of ion bombardment. Even when several fragments of an identical sample were set on the different sample holders, the intensity of lithium at saturation decreased gradually in the sequence of ion bombardment. It is uncertain at present what is responsible for the observed variance, but one of the possibilities is due to sample heating during ion bombardment because lithium is known to be mobile even at around room temperature in our glass [19]. For our SIMS measurements, therefore, only a single fragment of a sample was set at a time on the turn-table in order to reduce the possible heating effect.

Profile distortion, for example by inhomogeneous etching rate within the crater, sample heating during ion bombardment, or the deviation of the sputtering yield of secondary ions within ADR and AAR from that in the bulk as silicon profiles in Figs. 3 and 4 indicate, would reduce the reliability of the observed depth profiles. Nevertheless, in spite of these uncertainties, the observed ADR width for various samples was similar to the calculated width from TSPC. The calculation was made by assuming that the overall charge flowed during each TSPC run, Q_0, was carried solely by lithium ions entering the cathode region and that the same amount of lithium ions were depleted from the anode region.

Fig. 7 shows typical depth profiles of lithium and silver near the anode for the Ag–Au sample polarized up to 500 K, with Q_0 of 7.40×10^{-2} C cm^{-2}. The lithium profile on the cathode side of the same sample is shown in Fig. 8, which again shows evidence for lithium accumulation near the cathode. As expected, silver was not detected near the cathode. Accumulation of lithium at the

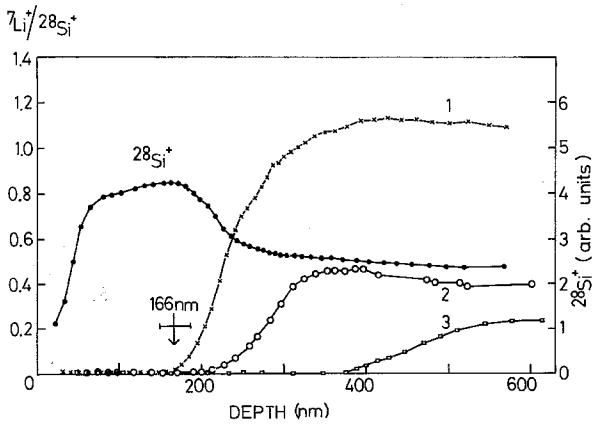

Figure 3 Depth profiles of lithium near the anode for polarized Au–Au (10) for three different spots on the surface. Calculated ADR width, with uncertainty due to inhomogeneous etching rate within the crater, is indicated by the arrow. Depth profile of silicon for the first spot is also shown.

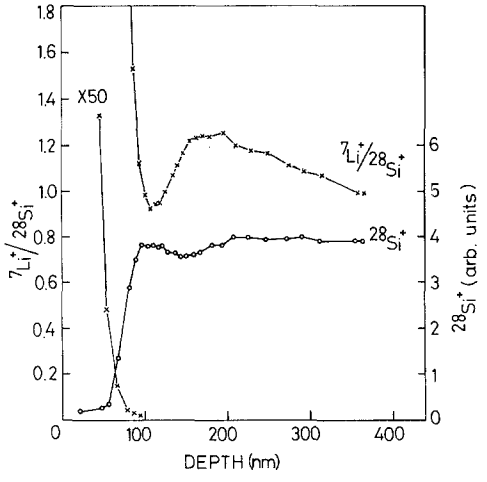

Figure 4 Depth profiles of lithium and silicon near the cathode for polarized Au–Au (10).

outside of ADR was observed for several samples with a silver anode (e.g. Fig. 7) but was absent for gold-anode samples. A similar type of accumulation of less mobile ions as potassium was reported for alkali-lead silicate glass [20]. If Q_0 was carried solely by lithium ions, the ADR width was estimated to be 247 nm, while was 140 nm or less from SIMS measurements. The difference in calculated and observed ADR width may be due, perhaps, to silver injection into glass from the anode.

4. Discussion

The closeness of the calculated and observed ADR width as well as the similarity of the TSPC slope to the reported activation energy for conduction suggests that, for gold-anode samples, gold would act as the totally blocking electrode in our experimental conditions of up to 500 K with an applied field of 200 V cm^{-1}, although SIMS measurements failed to give direct evidence concerning the blocking characteristics. Also, the closeness of the calculated and observed ADR width supports the hypothesis [11] that even localized alkali ions are depleted out of ADR by a high effective field within the region, although alkali depletion from the anode region was already demonstrated by capacitance [21] and ion-scattering spectrometric [20] studies as well as SIMS [8].

The TSDC current other than P2 seen in Fig. 2 may be due to back diffusion of space charge accumulated at either electrode or both. Some of lithium ions which reach the cathode during the conduction process are neutralized and penetrate into the cathode [22], while some tend to accumulate near the cathode. The closeness of the calculated and observed ADR width for gold-anode samples implies that every lithium ion which reaches the cathode can contribute 1.60×10^{-19} C to the external circuit, whether neutralized or unneutralized. Hence it is reasonable to assume that every lithium ion in AAR can contribute 1.60×10^{-19} C when it diffuses back to the bulk. If lithium ions in AAR were to be responsible for the TSDC current, the current should have been larger for the case a-a′ than for the case b-b′. On the other hand, a smaller Q_0 for the case b-b′ means thinner ADR width. So the lithium ions which diffuse back into ADR are easier to reach the anode for the case b-b′ than the case a-a′, giving larger TSDC current, at least in the low temperature range. A previous finding that space charge at AAR would relax by tunnelling rather than by thermal process [11] supports the present

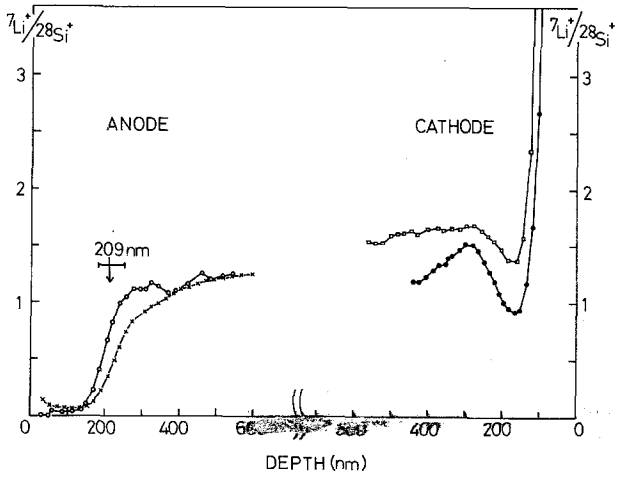

Figure 5 Depth profiles of lithium near the electrodes for the sample Au–Au (6) after polarizing it up to 500 K, where overall charge flowed during TSPC run was 6.25×10^{-2} C cm^{-2} which corresponds to the estimated ADR width of 209 nm.

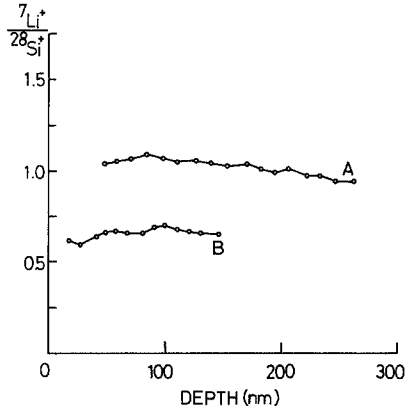

Figure 6 Depth profiles of lithium for previously unpolarized sample at two spots A and B 6 mm apart. Spot B was ion-etched after spot A.

speculation that the TSDC current, other than P2, may arise by the relaxation of space charge at ADR and not possibly by space charge at AAR.

Since silver ions are easy to migrate into glass, the silver anode–glass contact may be imagined to function as relatively ohmic, in the sense that lithium ions conduct to the cathode while the same amount of silver ions diffuse from the anode. In this scheme, space charge hardly develops near the electrodes and the Arrhenius plots for the TSPC curves should continue to be linear until silver is depleted out of the anode. This expectation was partly substantiated by the time-independent d.c. currents as observed when fired-on silver electrodes were used on glass [21, 23]. However, result 2 as mentioned above suggests the existence of more complicated phenomena at the interface.

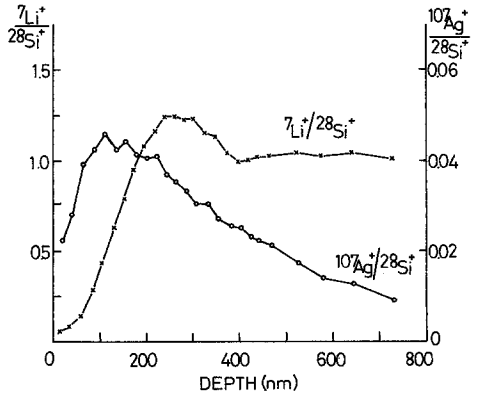

Figure 7 Depth profiles of lithium and silver near the anode for polarized Ag–Au (5) up to 500 K, where overall charge flowed during TSPC run was 7.40×10^{-2} C cm^{-2} which corresponds to the estimated ADR width of 247 nm if lithium is the only mobile species.

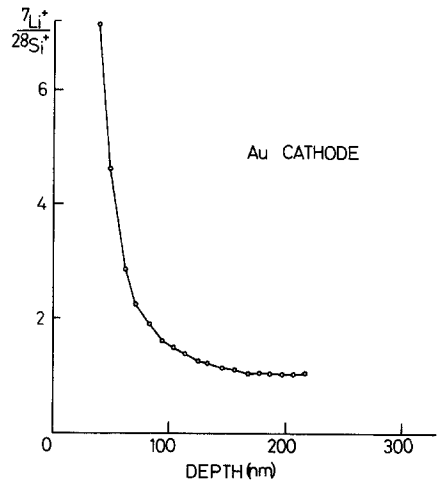

Figure 8 Depth profile of lithium on the cathode side of Ag–Au (5).

Silver was hardly observed visually on the silver-anode surfaces when the TSPC current suffered drastic degradation. The amount of our deposited silver corresponded to the charge of $(3 \sim 15) \times 10^{-2}$ C cm^{-2} if each silver ion can contribute 1.60×10^{-19} C to the external circuit at the instance of injection into glass. This amount of charge was at most several times larger than the charge flowed during TSPC runs for gold-anode samples. Therefore, it is possible that evaporated silver was depleted out of the anode at the instant the TSPC current suffered an abrupt change. Even after silver depletion out of the anode, the platinum foil would act as the anode so no depolarization current was found. The instability of the current after degradation, as mentioned in 3, may be due to incomplete contact between the platinum foil and the glass. However, for the sample where deposited silver was doubled intentionally or for the samples where silver paste rather than evaporated silver was used, the abovementioned current degradation was not so drastic and the current was still stable. Besides, silver remained in reasonable quantity on the anode surface even after the degradation.

The following is a tentative speculation on the observed current degradation even in the presence of remaining silver at the anode. It is generally believed that there exist the conduction paths for charge carriers in intrinsically heterogeneous structure of an amorphous material. Since the conduction characteristics was almost indifferent to the presence of striae (Table I), the conduction paths for lithium ions would be of microscopic

origin. Similarly, because of the heterogeneous structure of the anode material, there can be the preferential paths for silver movement. If some of the paths in the electrode are disconnected by the unsatisfactory contact between the rough surface of the sample and the anode, those silver ions beyond disconnection cannot move. Therefore, the situation becomes identical to that of silver depletion from the anode even when silver remains in reasonable quantity.

The profile of silver (Fig. 7) was different from that for thermal diffusion [5] in that the intensity of silver was relatively constant for a while, and gradually decreased afterwards. Deviation of the profiles from the usual diffusion characteristics of complementary error function shape was found also for the hydration of pre-irradiated silica glass [24]. If silver and lithium ions were to be mutually complementary in the conduction process, in the manner that silver ions occupy sites which previously were occupied by lithium ions, the calculated ADR width from Q_0 should have been identical with the observed one. Besides, the TSPC slope for silver-anode samples should have been identical with that for gold-anode ones. Therefore, Fig. 7 suggests that the available sites for charge carrier motion would be different for both species.

5. Conclusion

Gold can diffuse into SiO_2 [25] or $Li_2O \cdot 2SiO_2$ glass [5] when the temperature is 500° C or more. However, although no direct evidence was provided from SIMS, our TSPC data for gold-anode samples support the hypothesis that gold would act as the totally blocking electrode in our experimental conditions of up to 500 K with an applied field of 200 $V\,cm^{-1}$. On the other hand, the larger TSPC slope and rapid degradation of the TSPC current after the P3 peak maximum for silver-anode samples, as compared to gold-anode ones, suggest that silver can easily be injected into glass by the applied field. This is substantiated by SIMS. In view of the depth profiles for silver and lithium near the anode, it seems that both ions are not mutually complementary, but follow different paths for their conduction. Furthermore, it was concluded that the TSDC current, other than P2, may be due to back diffusion of space charge at ADR and not due to space charge at AAR.

Acknowledgements

Parts of the TSPC/TSDC measurements were made with the help of H. Suzuki of Nagoya Institute of Technology. Thanks are due to Professor K. Mizuno and C. Kato, Nagoya Institute of Technology, for permission and help with the crater-depth measurements. Valuable advice on the surface-charging effect given by Professor K. Takizawa of Niigata University is gratefully acknowledged.

References

1. D. E. CARLSON and C. E. TRACY, *J. Appl. Phys.* **46** (1975) 1575.
2. R. H. DOREMUS, *Phys. Chem. Glasses* **9** (1968) 128.
3. A. IINO and A. MIZUIKE, *Bull. Chem. Soc. Japan* **50** (1977) 1469.
4. Y. H. HAN, N. J. KREIDL and D. E. DAY, *J. Non-Cryst. Solids* **30** (1979) 241.
5. C. KIM and M. TOMOZAWA, *J. Amer. Ceram. Soc.* **59** (1976) 321.
6. E. L. MILNE and P. GIBBS, *J. Appl. Phys.* **35** (1964) 2364.
7. G. W. ARNOLD and J. A. BORDERS, *ibid.* **48** (1977) 1488.
8. R. G. GOSSINK, *Glass Technol.* **21** (1980) 125.
9. J. VANDERSCHUEREN and J. GASIOT, in "Thermally Stimulated Relaxation in Solids", edited by P. Braunlich (Springer, Berlin, 1979) p. 135.
10. A. DOI, *J. Mater. Sci.* **17** (1982) 2087.
11. *Idem, Jap. J. Appl. Phys.* **22** (1983) 228.
12. A. DOI and D. E. DAY, *J. Appl. Phys.* **52** (1981) 3433.
13. D. V. McCAUGHAN and R. A. KUSHNER, in "Characterization of Solid Surfaces", edited by P. F. Kane and G. B. Larrabee (Plenum Press, New York, 1974) p. 627.
14. R. G. GOSSINK, H. A. M. de GREFTE and H. W. WERNER, *J. Amer. Ceram. Soc.* **62** (1979) 4.
15. M. KOBAYASHI, PhD thesis, Tokyo Institute of Technology (1980).
16. R. J. CHARLES, *J. Amer. Ceram. Soc.* **46** (1963) 235.
17. H. NAMIKAWA, *J. Non-Cryst. Solids* **18** (1975) 173.
18. J. A. McHUGH, in "Methods and Phenomena-Method of Surface Analysis", edited by A. W. Czanderna (Elsevier, Amsterdam, 1975) p. 233.
19. J. R. HENDRICKSON and P. J. BRAY, *J. Chem. Phys.* **61** (1974) 2754.
20. D. E. CARLSON, K. W. HANG and G. F. STOCKDALE, *J. Amer. Ceram. Soc.* **57** (1974) 291.
21. G. WALLIS, *ibid.* **53** (1970) 563.
22. K. TAKIZAWA, *ibid.* **61** (1978) 475.
23. K. HUGHES and J. O. ISARD, *Phys. Chem. Glasses* **9** (1968) 37.
24. C. BURMAN and W. A. LANFORD, *J. Appl. Phys.* **54** (1983) 2312.
25. T. W. HICKMOTT, *ibid.* **51** (1980) 4269.

Received 6 June
and accepted 6 July 1984